Electronic Supplementary Material (ESI) for Polymer Chemistry.

Supporting Information

The effect of side chain spacer length on the thermoresponsive behavior of poly(methylamide acrylate)s

Alexander Rajakanthan[a], Paul Wilson [b]* and Kristian Kempe [a,c]*

[a] Monash Institute of Pharmaceutical Sciences, Monash University, 381 Royal Parade, Parkville VIC 3052, Australia

[b] Department of Chemistry, The University of Warwick, CV4 7AL, United Kingdom

[c] Department of Material Science and Engineering, Monash University, Clayton, VIC 3800, Australia

Equation S1. Mathematic equation to calculate monomer self-association calculating, K_a.

$$\Delta\delta_{obs} = \frac{\Delta\delta_{max}\left\{(2[M] + K_d) - [(2[M] + K_d)^2 - 4[M]^2]^{\frac{1}{2}}\right\}}{2[M]}$$

Where $K_d = [M]^2/[D]$ and $K_a = 1/K_d$. K_d, [M] and [D] are dissociation constants, monomer and dimer concentrations (mol L^{-1}, M) respectively.

Table S1. RAFT conditions used to prepare poly(methylamide acrylate) homopolymers (time: 24 h).

Sample	Target DP	Conversion (%)	[M] (mol L^{-1})	[BCTP] (mol L^{-1})	[tBuOOH] (µmol L^{-1})	[AsAc] (µmol L^{-1})
$P(MAmEA)_{100}$	100	100	3.09	0.031	7.7	3.9
$P(MAmPA)_{97}$	100	97	3.09	0.031	7.7	3.9
$P(MAmBA)_{25}$	25	100	3.09	0.124	30.9	15.5
$P(MAmBA)_{48}$	50	96	3.09	0.062	15.5	7.7
$P(MAmBA)_{99}$	100	99	3.09	0.031	7.7	3.9
$P(MAmBA)_{190}$	200	95	3.09	0.015	3.9	1.9

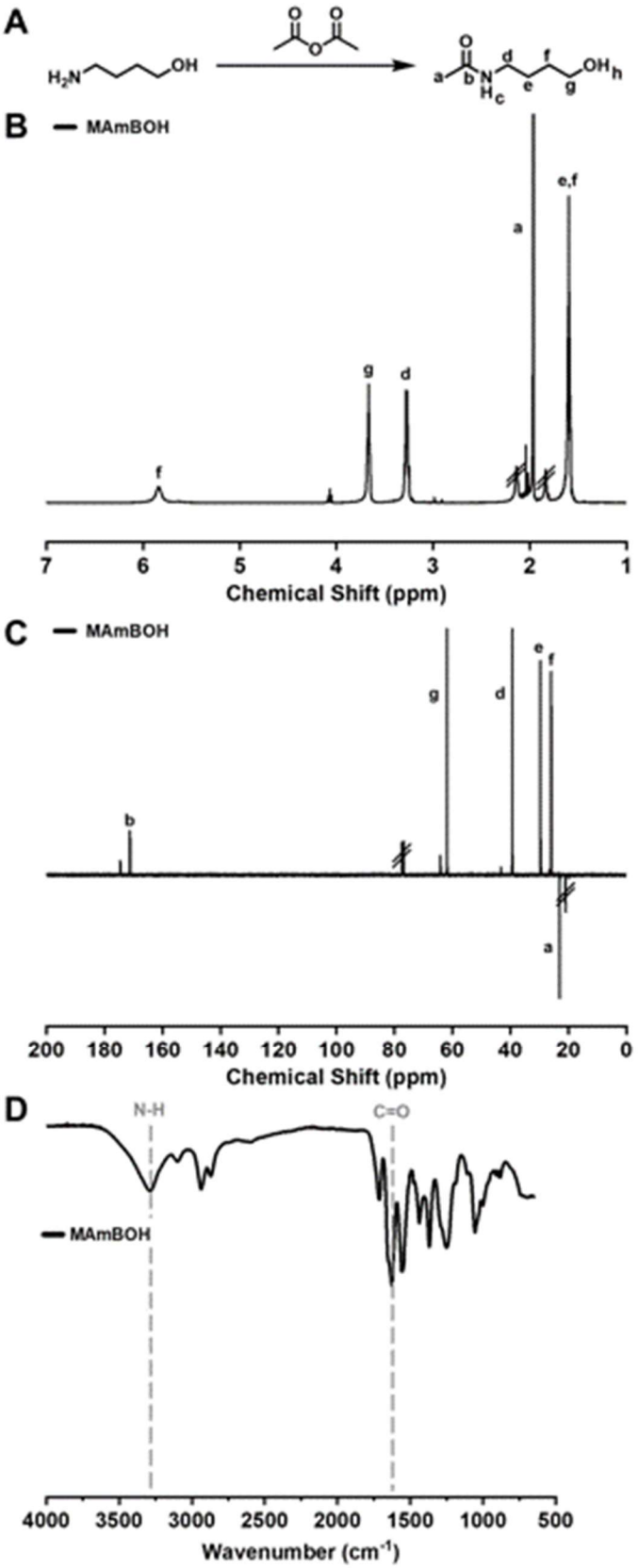

Figure S1. (A) Synthesis pathway of MAmBOH; (B) ^{1}H NMR spectrum (400 MHz, $CDCl_3$) of MAmBOH; (C) ^{13}C NMR spectrum (400 MHz, $CDCl_3$) of MAmBOH; (D) FT-IR spectrum of MAmBOH.

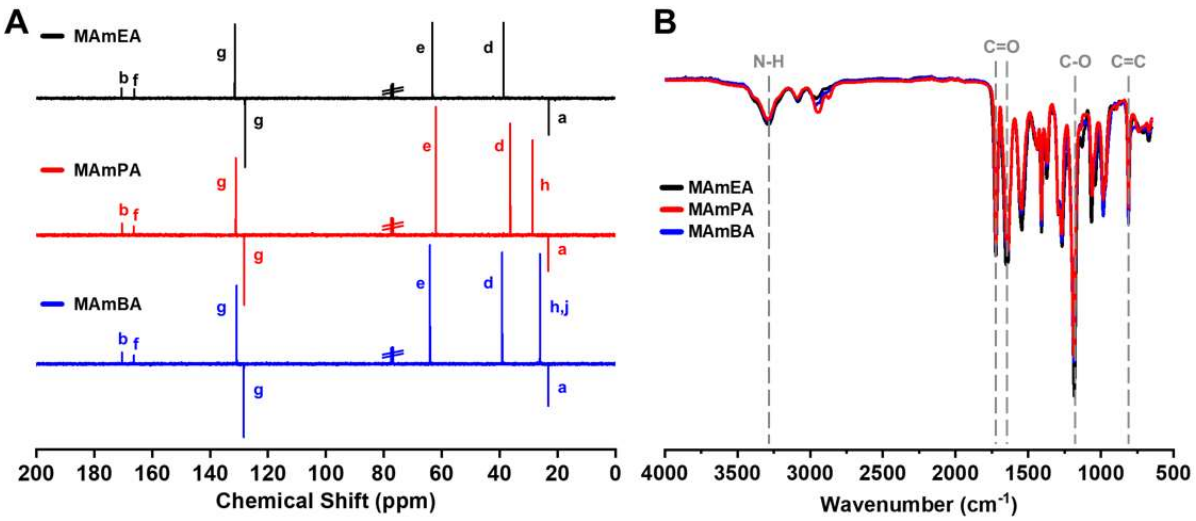

Figure S2. (A) ^{13}C NMR spectra (400 MHz, $CDCl_3$) of MAmEA, MAmPA and MAmBA; (B) FT-IR spectra of MAmEA, MAmPA and MAmBA.

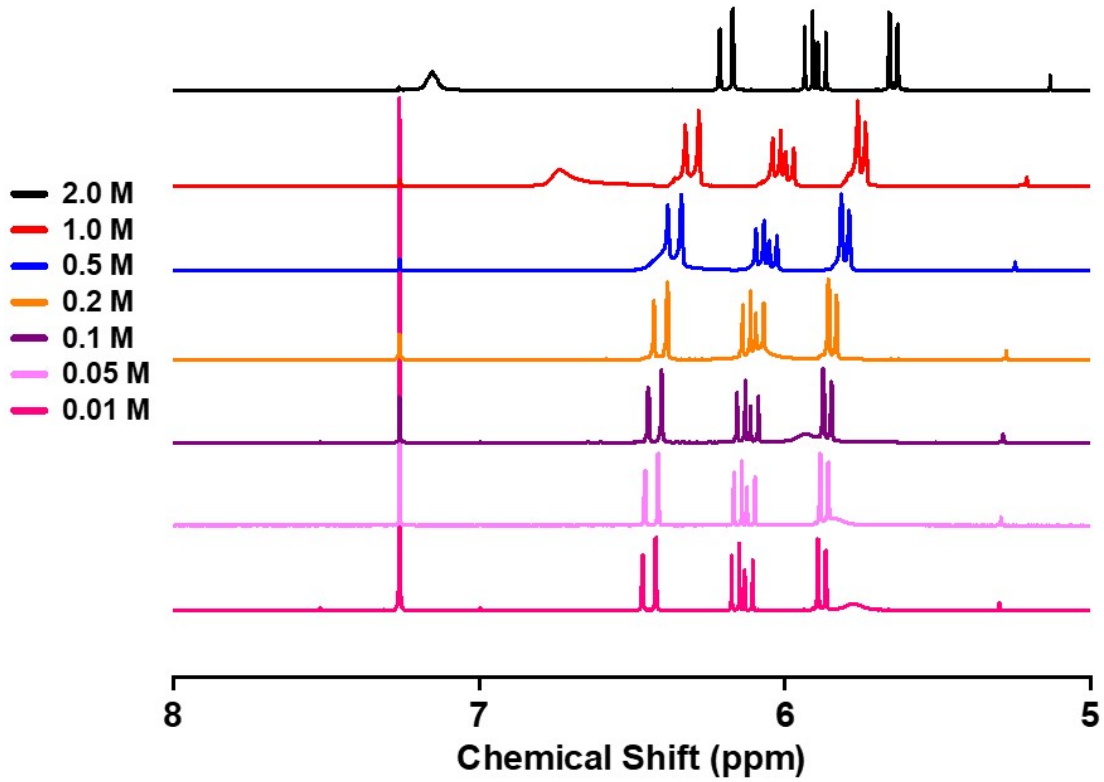

Figure S3. ^{1}H NMR spectra (400 MHz, $CDCl_3$) of MAmEA at varying [M], highlighting the concentration-dependent change in chemical shift of H_c.

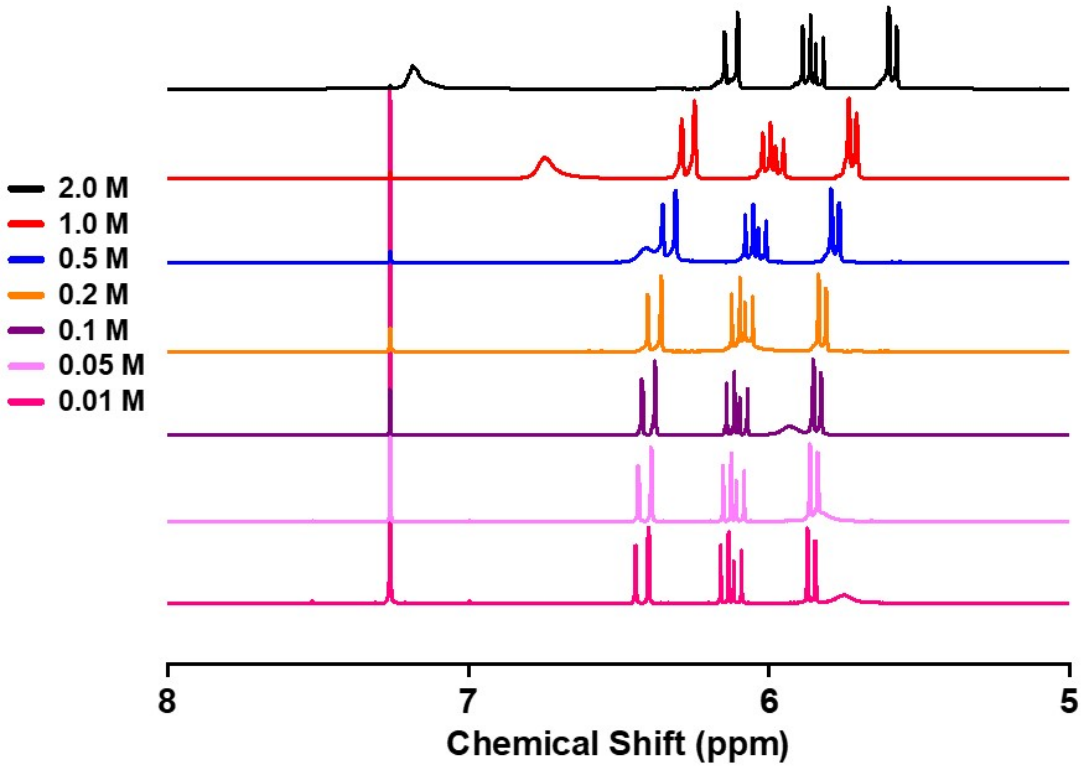

Figure S4. ^{1}H NMR spectra (400 MHz, $CDCl_3$) of MAmPA at varying [M], highlighting the concentration-dependent change in chemical shift of H_c.

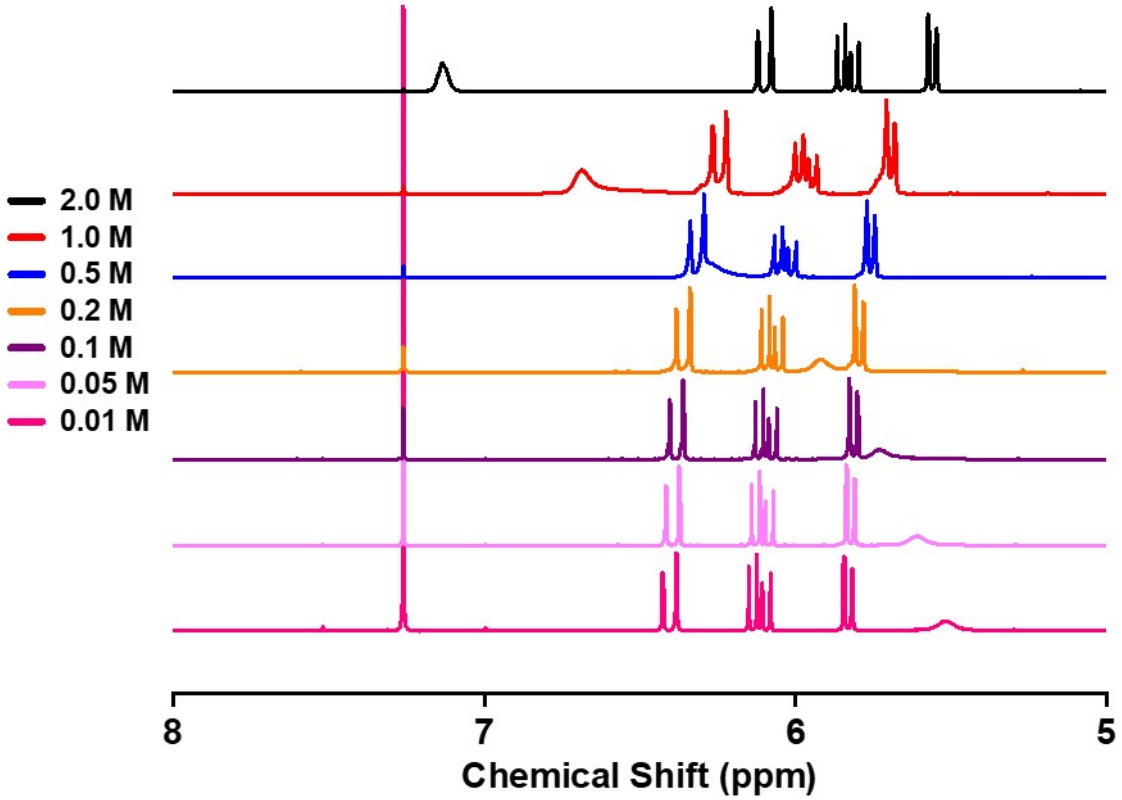

Figure S5. ^{1}H NMR spectra (400 MHz, $CDCl_3$) of MAmBA at varying [M], highlighting the concentration-dependent change in chemical shift of H_c.

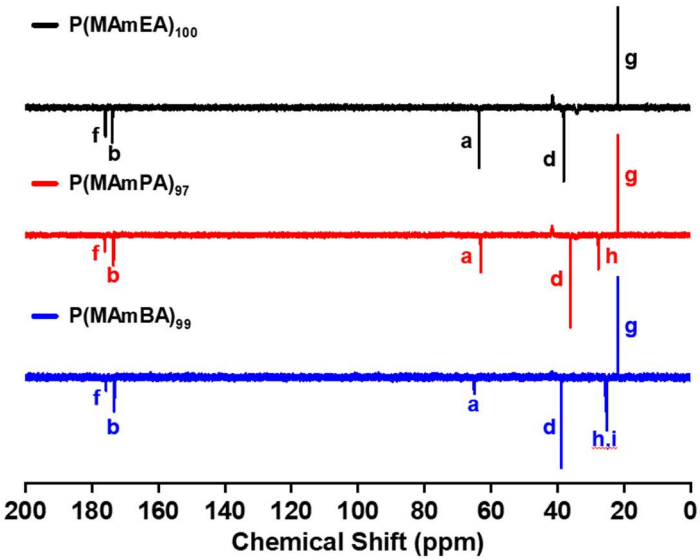

Figure S6. ^{13}C NMR spectra (400 MHz, D_2O) of $P(MAmEA)_{100}$, $P(MAmPA)_{97}$ and $P(MAmBA)_{99}$.

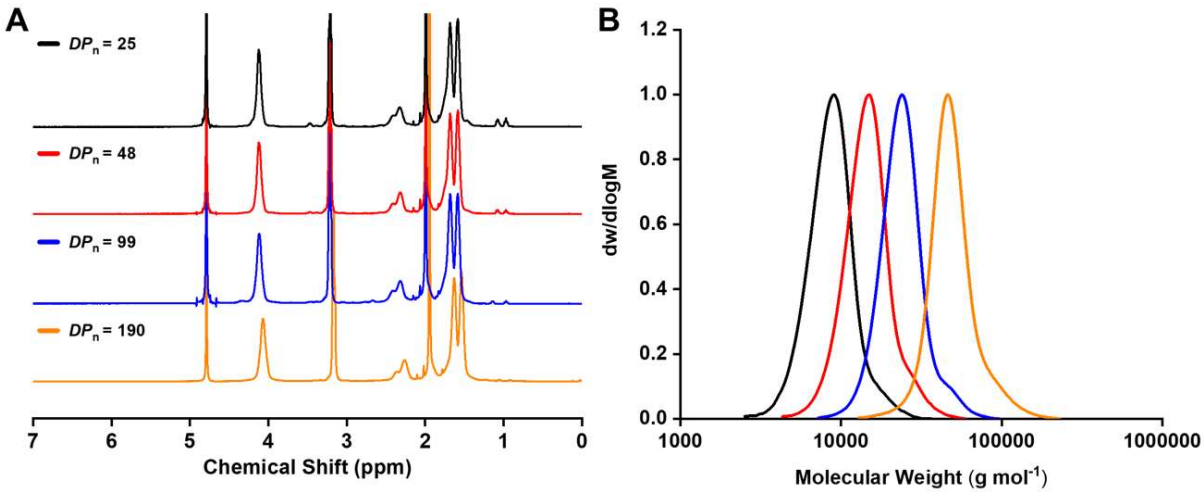

Figure S7. (A) ^1H NMR spectra (400 MHz, D_2O) of $P(MAmBA)_{25}$, $P(MAmBA)_{48}$, $P(MAmBA)_{99}$ and $P(MAmBA)_{190}$; (B) SEC traces of $P(MAmBA)_{25}$ (M_n = 8,200, $Đ_M$ = 1.12), $P(MAmBA)_{48}$ (M_n = 12,800, $Đ_M$ = 1.12), $P(MAmBA)_{99}$ (M_n = 22,700, $Đ_M$ = 1.11) and $P(MAmBA)_{190}$ (M_n = 48,300, $Đ_M$ = 1.12).

Table S2. Conditions used for turbidity measurements of P(MAmBA) and the associated cloud point temperatures (T_{cp}). Temperature range measured: 30 - 80 °C.

DP_n	Concentration (mg ml^{-1})	Media	T_{cp} (° C)
190	5	PBS	39.6
99	5	PBS	52.8
48	5	PBS	66.0
25	5	PBS	N/A
99	1	PBS	57.2
99	0.1	PBS	N/A
99	5	0.137 M NaCl	59.6
99	5	Milli-Q Water	65.8

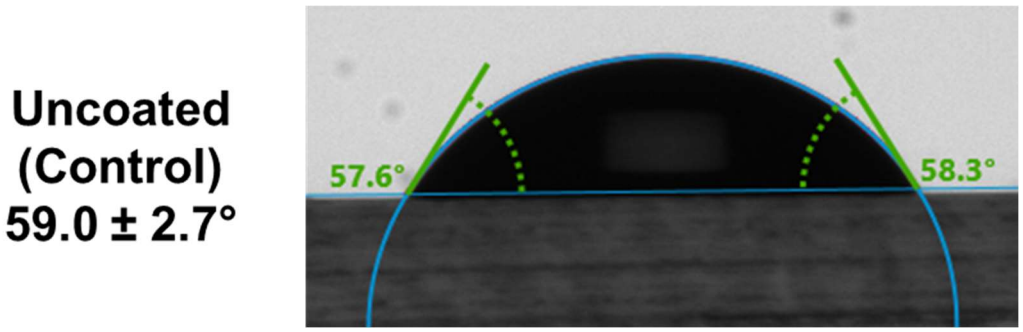

Figure S8. Water contact angle image of an uncoated glass slide.